

# Error Analysis of time-based and angle-based location methods

\*Dong-Hyoun Kim<sup>1</sup>, Seung-Hun Song<sup>2</sup>, Tae-Kyung Sung<sup>3</sup>

<sup>1</sup> Dept. of Information and Communication Engr., Chungnam Nat'l Univ. (E-mail: oneoctave@ivlab.cnu.ac.kr)

<sup>2</sup> Dept. of Information and Communication Engr., Chungnam Nat'l Univ. (E-mail: lspheonix@hanafos.com)

<sup>3</sup> Faculty of Electric and Computer Engr., Chungnam Nat'l Univ. (E-mail: tksaint@cnu.ac.kr)

## Abstract

Indoor positioning is recently highlighted and various kinds of indoor positioning systems are under developments. Since positioning systems have their own characteristics, proper positioning scheme should be chosen according to the required specifications. Positioning methods are often classified into time-based and angle-based one, and this paper presents the error analysis of these location methods. Because measurement equations of these methods are nonlinear, linearization is usually needed to get the position estimate. In this paper, Gauss-Newton method is used in the linearization. To analyze the position error, we investigate the error ellipse parameters that include eccentricity, rotation angle, and the size of ellipse. Simulation results show that the major axes of error ellipses of TOA and AOA method lie in different quadrants at most region of workspace, especially where the geometry is poor. When the TOA/AOA hybrid scheme is employed, it is found that the error ellipse is reduced to the intersection of ellipses of TOA and AOA method.

**Keywords:** Gauss-Newton method, TOA, TDOA, AOA, Hybrid method

## 1. Introduction

Positioning systems based on GPS exist to guide users in outdoor environments where GPS works. In case of indoor environment such as office and home, however, GPS signal is blocked and the users cannot get their position. Recently, various kinds of alternatives for indoor positioning are under developments using UWB (Ultra Wide-Band), IR (Infra-Red), Ultra-Sonics, RFID (Radio Frequency Identification), WLAN (Wireless LAN), and so on [1].

There are several kinds of positioning methods in the literature; TOA (Time Of Arrival), TDOA (Time Difference Of Arrival), AOA (Angle Of Arrival), RSS (Received Signal Strength), and their hybrid systems [1]. In TOA method, the distance between tag and sensor is determined from the measured one-way propagation time of the signal traveled. In the TDOA method, the differences in arrival time of multiple pairs of sensors are measured at the tag. Time-based methods need highly accurate time synchronization between sensors. Therefore, performance of positioning system is influenced by the synchronization accuracy. In AOA method, sensors should have an array antenna to measure the arrival angles of the signal transmitted from a tag. AOA method does not require the time synchronization between sensors. In general, hybrid methods combine the time-based and angle-based method together.

This paper presents the error analysis of positioning methods. Since the measurement equations of TOA, TDOA, and AOA methods are nonlinear, linearization is commonly employed to estimate the tag position. GN (Gauss-Newton) algorithm is used in this paper in estimating the position. To analyze the performance of positioning method, the error ellipse obtained from the error covariance is often used. It is known that the position estimate and its error covariance obtained by GN algorithm in TOA method are completely equal to those in TDOA method [2]. Therefore, this paper only compares the performance of TOA and AOA method.

Time-based and angle-based location methods have different shape of error ellipses. Therefore, we can predict the

performance improvement of the TOA/AOA hybrid system by analyzing the error ellipses of TOA and AOA method. By computer simulation, we analyze the error ellipses of two methods at all grid points in the work space, and then compare them to that of the hybrid system.

## 2. Positioning Algorithm

### 2.1 Measurement Models

Let  $\mathbf{x} = [x \ y]^T$  be the tag position to be determined and the known coordinates of the  $i$ -th sensor be  $\mathbf{x}_i = [x_i \ y_i]^T$ ,  $i=1, 2, \dots, m$ , where  $m$  is the total number of sensors transmitting/receiving signals to/from the tag.

TOA is the one-way propagation time taken for the signal to travel to the tag. The pseudo-range measurement is obtained from the travel time and its equation is given by [3][4]

$$r_i = \sqrt{(x_i - x)^2 + (y_i - y)^2} + c \cdot b + v_{ri} \quad (1)$$

where  $c$  is the speed of light,  $b$  is receiver clock bias, and  $v_{ri}$  is a measurement noise. It is assumed that the measurement noises are i.i.d. (independently and identically distributed) white Gaussian with variance  $\sigma_i^2$ .

2D AOA measurement is azimuth angle between sensor and tag. It is obtained from the path difference between received signals at the array antenna of a sensor as shown in Fig. 1 [5]. If the orientation of array antennas is not coincided with the reference frame, azimuth angle should have an offset. When the array antenna is installed as shown in Fig. 1, azimuth angle  $\alpha_i$  is given by

$$\alpha_i = \alpha_{off}^i + \alpha_{ri} \quad (2)$$

where  $\alpha_{off}^i$  is an offset and  $\alpha_{ri}$  is the angle measured at the antenna.

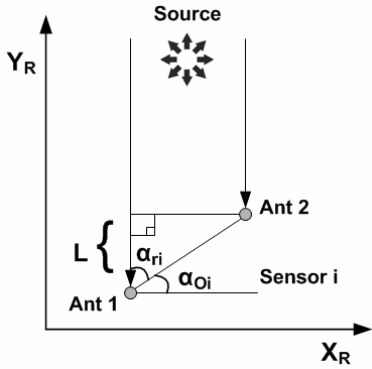


Fig. 1 Array Antenna for AOA

Using the sensor and tag position in reference frame, azimuth angle can be represented as [6][7]

$$\tan(\alpha_i) = \frac{y - y_i}{x - x_i} \quad (3)$$

Considering measurement noise, relationship between the angle measurement and path difference at the antenna array is given by

$$d \cos(\alpha_{ri} + v_{ai}) = L_i + v_{li} \quad (4)$$

where  $d$  is the distance between antennas and  $L_i$  is the path difference.  $v_{ai}$ ,  $v_{li}$  are noises in  $\alpha_{ri}$  and  $L_i$  respectively. If  $v_{li}$  is i.i.d. white Gaussian with variance  $\sigma_a^2$ , angle measurement and its noise are written as

$$f_i = \alpha_i + v_{ai} \quad (5)$$

$$v_{ai} \approx N\left(0, \frac{\sigma_a^2}{d^2 \sin^2 \alpha_{ri}}\right)$$

## 2.2 Gauss-Newton Method

Linearized equation of GN method for TOA positioning is given by [8][9]

$$\delta \mathbf{r} = \mathbf{H}_t \delta \mathbf{x}_t + \mathbf{w}_t \quad (6)$$

$$\delta \mathbf{r} = \begin{bmatrix} r_1 - r_{01} \\ r_2 - r_{02} \\ \vdots \\ r_m - r_{0m} \end{bmatrix} \mathbf{H}_t = \begin{bmatrix} \frac{\partial r_1}{\partial x} & \frac{\partial r_1}{\partial y} \\ \frac{\partial r_2}{\partial x} & \frac{\partial r_2}{\partial y} \\ \vdots & \vdots \\ \frac{\partial r_m}{\partial x} & \frac{\partial r_m}{\partial y} \end{bmatrix} \delta \mathbf{x}_t = \begin{bmatrix} x - x_0 \\ y - y_0 \\ b - b_0 \end{bmatrix} \mathbf{w}_t = \begin{bmatrix} v_{r1} \\ v_{r2} \\ \vdots \\ v_{rm} \end{bmatrix}$$

where  $(x_0, y_0)$  is nominal point and  $r_{0i}$  is the distance between sensor and the nominal point. GN method determines the position perturbation by simply solving Eq.(6) using least square.

$$\delta \hat{\mathbf{x}}_t = (\mathbf{H}_t^T \mathbf{H}_t)^{-1} \mathbf{H}_t^T \delta \mathbf{r} \quad (7)$$

From Eq. (7), the tag position is given by

$$\hat{\mathbf{x}}_t = \mathbf{x}_0 + \delta \hat{\mathbf{x}}_t \quad (8)$$

Final estimate is obtained by repeating Eq.(7) and (8) until the tag position converges.

Linearized equation for AOA method is written as [7]

$$\delta \mathbf{f} = \mathbf{H}_a \delta \mathbf{x}_a + \mathbf{w}_a \quad (9)$$

$$\delta \mathbf{f} = \begin{bmatrix} f_1 - \alpha_{01} \\ f_2 - \alpha_{02} \\ \vdots \\ f_m - \alpha_{0m} \end{bmatrix} \mathbf{H}_a = \begin{bmatrix} \frac{\partial f_1}{\partial x} & \frac{\partial f_1}{\partial y} \\ \frac{\partial f_2}{\partial x} & \frac{\partial f_2}{\partial y} \\ \vdots & \vdots \\ \frac{\partial f_m}{\partial x} & \frac{\partial f_m}{\partial y} \end{bmatrix} \delta \mathbf{x}_a = \begin{bmatrix} x - x_0 \\ y - y_0 \end{bmatrix} \mathbf{w}_t = \begin{bmatrix} v_{a1} \\ v_{a2} \\ \vdots \\ v_{am} \end{bmatrix}$$

where  $\alpha_{0i}$  is azimuth angle between  $i$ -th sensor and nominal user. Using Eq. (9), position estimate of AOA method is obtained by the similar manner to TOA method. Note that the weighted least square should be employed in this case since the variance of angle measurement noise is varying according to the azimuth angle of the corresponding sensor as in Eq. (5).

In TOA/AOA hybrid method, Eq. (6) and (9) are augmented to get a single linear equation. Weighted least square is either used in this case to get the estimate.

## 2.3 Error Ellipse

In radio-navigation, position estimates are influenced by the geometry of sensors to constitute the position error ellipse. We will analyze the error ellipses of time-based and angle-based location method. Two-dimensional error ellipse is plotted in Fig. 2. The  $\sigma_L$  and  $\sigma_S$  are major and minor axis of error ellipse respectively.  $\theta$  is the inclination of major axis in reference frame. Relationship between the covariance matrix of estimation error and the parameters of error ellipse is given by [3]

$$\text{cov}(\hat{\mathbf{x}}) = \begin{bmatrix} \sigma_x^2 & \sigma_{xy} \\ \sigma_{xy} & \sigma_y^2 \end{bmatrix} = \begin{bmatrix} \cos \theta & -\sin \theta \\ \sin \theta & \cos \theta \end{bmatrix} \begin{bmatrix} \sigma_L^2 & 0 \\ 0 & \sigma_S^2 \end{bmatrix} \begin{bmatrix} \cos \theta & \sin \theta \\ -\sin \theta & \cos \theta \end{bmatrix} \quad (10)$$

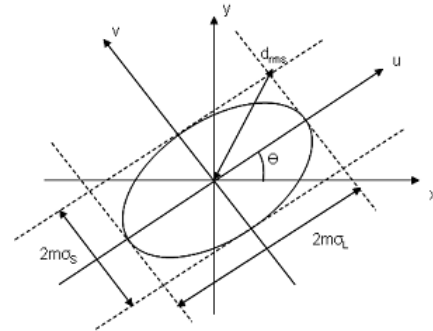


Fig. 2. The error ellipse

In case of TOA method, from Eq. (7), covariance matrix of estimation error is written as

$$\text{cov}(\hat{\mathbf{x}}_t) = \sigma_t^2 \cdot (\mathbf{H}_t^T \mathbf{H}_t)^{-1} \quad (11)$$

Covariance matrix of measurement noises of AOA method in Eq. (5) is represented as

$$\text{cov}(\mathbf{w}_a) = \mathbf{Q}_a = \frac{\sigma_a^2}{d^2} \begin{bmatrix} 1/\sin^2(\alpha_{r1}) & 0 & \cdots & 0 \\ 0 & 1/\sin^2(\alpha_{r2}) & \cdots & 0 \\ \vdots & \vdots & \ddots & \vdots \\ 0 & 0 & \cdots & 1/\sin^2(\alpha_{rm}) \end{bmatrix} \quad (12)$$

Consequently, covariance matrix of estimation error for AOA method is given by

$$\text{cov}(\hat{\mathbf{x}}_a) = (\mathbf{H}_a^T \mathbf{Q}_a^{-1} \mathbf{H}_a)^{-1} \quad (13)$$

It is known that the major axis, minor axis, and inclination of error ellipse are obtained from error covariance matrix that is given by [10]

$$\tan(2\theta) = \frac{2\sigma_{xy}}{\sigma_x^2 - \sigma_y^2}, \quad 0 \leq \theta \leq \frac{\pi}{2} \quad (14)$$

$$\sigma_L^2 = 0.5 \left[ \sigma_x^2 + \sigma_y^2 + \sqrt{(\sigma_x^2 - \sigma_y^2)^2 + 4\sigma_{xy}^2} \right]$$

$$\sigma_S^2 = 0.5 \left[ \sigma_x^2 + \sigma_y^2 - \sqrt{(\sigma_x^2 - \sigma_y^2)^2 + 4\sigma_{xy}^2} \right]$$

When we compute  $\theta$ , two possible solutions always exist. This ambiguity can be solved by [10]

$$\theta = \frac{1}{2} \tan^{-1} \left( \frac{2\sigma_{xy}}{\sigma_x^2 - \sigma_y^2} \right) + i \cdot \frac{\pi}{2}, \quad 0 \leq \theta - i \cdot \frac{\pi}{2} \leq \frac{\pi}{2}, \quad i = 0, 1 \quad (15)$$

$$i = \begin{cases} 0, & \frac{\sigma_{xy}}{\sigma_x^2} > 0 \\ 1, & \frac{\sigma_{xy}}{\sigma_x^2} < 0 \end{cases}$$

To analyze the performance of location methods, size of error ellipse is also an important factor. In this paper, measure of ellipse size is chosen as

$$S = 4\sqrt{\sigma_L^2 \cdot \sigma_S^2} \quad (16)$$

### 3. Simulation Results

In computer simulation, workspace is assumed to be 12 by 12[m]. Position estimate is analyzed at every grid point, and the distance between two adjacent grid points is 1[m] in x- and y-axis direction. When the estimate converges within  $10^{-2}$ [m], the iteration is terminated. It is assumed that the sensors are installed to make 'L' shape as shown in Fig. 3 and their coordinates are given by (-6, 6)[m], (6, 6)[m], (6, -6)[m], and (0, 6)[m].

AOA measurement noise is generated using Eq. (5).  $\sigma_r^2$  (variance of TOA noise) and  $\sigma_a^2$  in Eq. (5) are given  $10^{-2}$ [m] and  $10^{-4}$ [m] respectively so that two methods may have almost the same size of error ellipse at the center of workspace. No multipath environment is assumed. At every grid point, 100 trials are repeated for Monte Carlo simulation to get the standard deviation of the estimation error, divergence rate, and convergence speed.

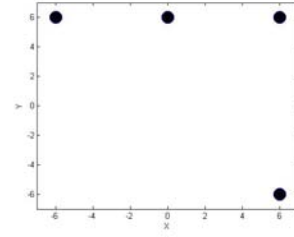
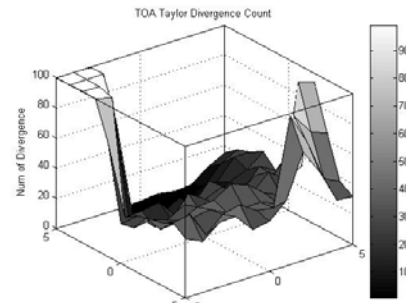
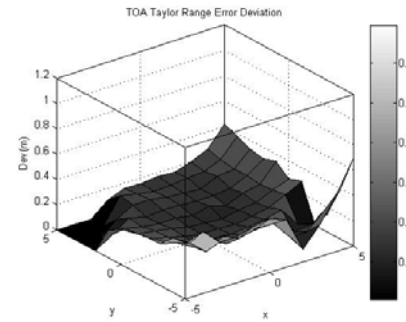


Fig. 3. Sensor geometry

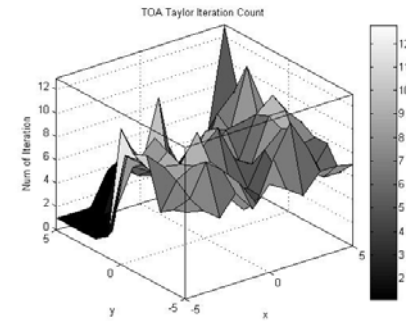
Simulation results of TOA method are plotted in Fig. 4. More than 10 trials are diverged at almost everywhere of the workspace. Especially when the tag is located near (-5, 5), all the trials diverge due to the poor geometry. Standard deviation of estimation error is computed using the outputs of trials converged only. At the center of the work space, standard deviation is about 0.2m. As the tag moves to the edges, standard deviation increases as shown Fig. 4 (b). The average number of iterations is 5~10 at most of the work space.



(a) The Number of Divergence



(b) Standard Deviation

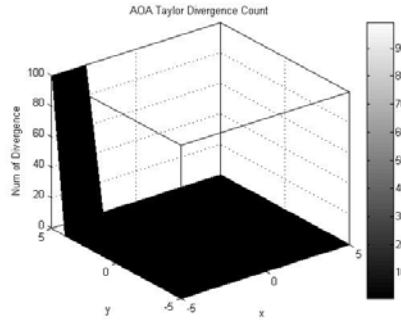


(c) The Number of Iterations

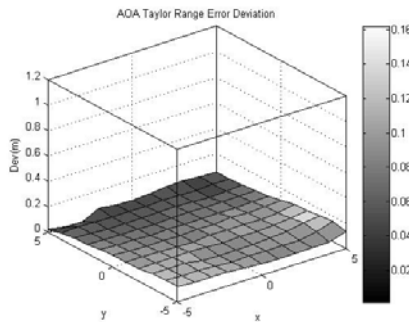
Fig. 4. Simulation results of TOA

Simulation results of AOA method are plotted in Fig. 5. Divergence takes place only at (-5, 5), while it does almost everywhere in TOA. Furthermore, standard deviation of estimation error of AOA is smaller than that of TOA at all grid

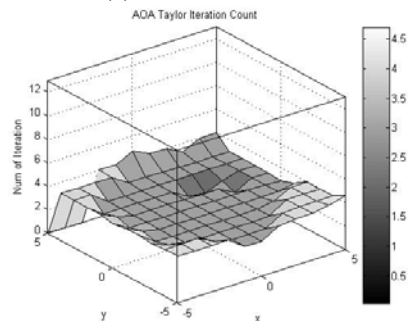
points. It may be because the minimum number of sensors for AOA method is just 2 in 2D case, while that of TOA method is 3. It is known that the performance of GN method is improved as the number of sensors increases. Standard deviation of estimation error becomes somewhat larger at left-lower side of workspace shown in Fig. 3 where the sensor geometry is poor. The number of iterations is 2~4, which is better than TOA method. Note that the estimation error and the iteration become larger if the number of sensors is 3.



(a) The Number of Divergences



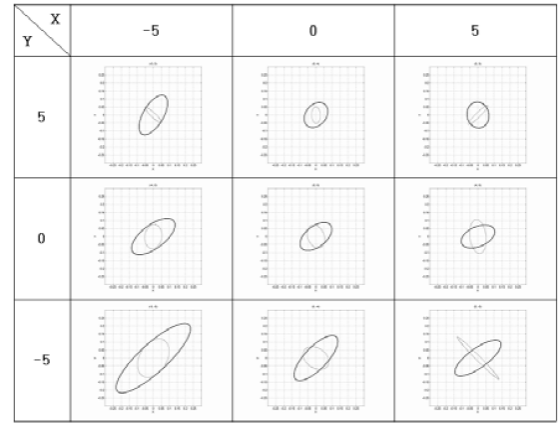
(b) Standard Deviation



(c) The Number of Iterations

Fig. 5. Simulation results of AOA

Next, we analyze the parameters of error ellipses of AOA and TOA method at all grid points using Eq. (11) and Eqs. (13)~(16). Shape of ellipses and their parameters at 9 grid points are shown as shown in Fig. 6 and Table 1 respectively. In the figure, the major axes of TOA and AOA method lie in different quadrants at most region of workspace. In both TOA and AOA method, size of ellipse is biggest when the tag position of tag is (-5, -5). It means that the size of error ellipse becomes larger when the geometry is poor. Eccentricity is smallest when the tag is (5, 5) for TOA and (0, -5) for AOA. Standard deviation of eccentricity at all grid points is 0.153 in AOA, while 0.103 in TOA. This means that the sharpness of ellipse in AOA is changed 20% larger compared to TOA. Standard deviation of size of ellipse is 0.016 in AOA and 0.02 in TOA, which means that size of the ellipse varies 25% more in TOA method compared to AOA.



— : TOA ... : AOA  
Fig. 6. Error ellipses of TOA and AOA

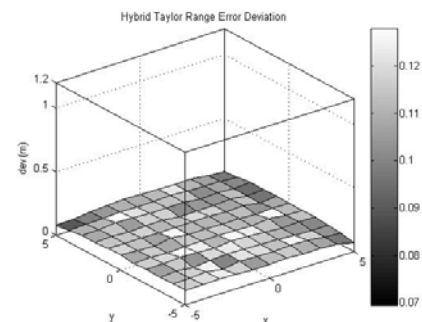
Table 1. Parameters of error ellipses of TOA and AOA

Y \ X	-5		0		5		
	AOA	TOA	AOA	TOA	AOA	TOA	
5	$\theta$	136.7	59.4	90.3	54.9	44.3	101.8
	e	0.979	0.889	0.963	0.642	0.986	0.542
	i	1	0	1	0	0	1
	S	0.031	0.094	0.027	0.073	0.035	0.075
0	$\theta$	71.49	34.11	112.5	38.06	94.68	17.95
	e	0.734	0.909	0.722	0.830	0.924	0.851
	i	0	0	1	0	1	0
	S	0.068	0.119	0.062	0.086	0.085	0.086
-5	$\theta$	59.87	42.72	159.0	50.28	134.7	33.74
	e	0.757	0.957	0.639	0.938	0.997	0.936
	i	0	0	1	0	1	0
	S	0.105	0.164	0.078	0.125	0.051	0.102

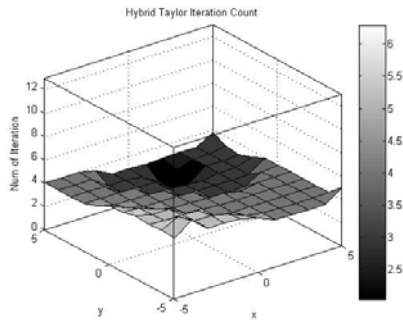
※  $\theta$  : rotation angle( $^{\circ}$ ), e : eccentricity, i : ambiguity, S : area

Because TOA and AOA method show different error characteristics, it is expected that the performance is improved if two methods combine together. Now, we analyze the performance of TOA/AOA hybrid method and compared it to that of standalone TOA and AOA.

Monte Carlo simulation results of hybrid TOA/AOA are plotted in Fig. 7. There exists no trial diverged all over the workspace. Standard deviation of estimation error of TOA/AOA hybrid method is smaller than that of standalone TOA or AOA at all grid points. Furthermore, standard deviation is almost unchanged at entire work space, which means that error performance is hardly changed according to the sensor geometry. The number of iterations is 2~4, which is similar to AOA method.



(a) Standard Deviation



(b) The Number of Iterations  
Fig. 7. Simulation results of Hybrid TOA/AOA

Finally, we analyze error ellipse of hybrid TOA/AOA and compare the results to those of standalone TOA and AOA method. Shape of ellipse at 9 grid points is shown in Fig. 8. Error ellipse of hybrid TOA/AOA is almost same to the intersection of two ellipses in Fig. 6. Because the major axes of standalone TOA and AOA lie in different quadrants at most of workspace, the size of ellipse is drastically reduced. Consequently, performance of TOA/AOA hybrid method is greatly improved as it is known.

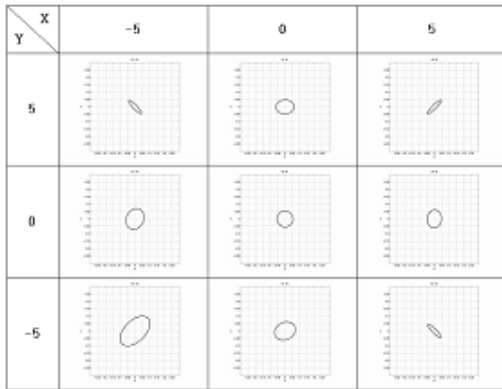


Fig. 8. Error Ellipse of Hybrid TOA/AOA

#### 4. Conclusion

Time-based and angle-based location method show different error performance. This paper presents the performance comparison of TOA, AOA, and their hybrid using computer simulation and error ellipse analysis. Eccentricity of AOA method is larger than TOA method, especially where the geometry is poor. Size of ellipse is changed more in TOA compared to AOA. Since the error ellipse of hybrid TOA/AOA is almost same to the intersection of two ellipses by standalone TOA and AOA, performance of TOA/AOA hybrid method is greatly improved compared to the standalone methods.

#### Acknowledgement

This research was supported by the Program for the Training of Graduate Students in Regional Innovation which was conducted by the Ministry of Commerce Industry and Energy of the Korean Government and MIC & IITA through IT Leading R&D Support Project

#### Reference

1. Oppermann, M. Hämäläinen, J. Iinatti, "UWB Theory and Applications", John Wiley & Sons Ltd, Chichester, 2004.
2. D.H. Shin and T.K. Sung, "Comparisons of Error Characteristics between TOA and TDOA positioning", IEEE Transactions on Aerospace and Electronic Systems, Vol. 38, no. 1, pp. 307-311, Jan 2002.
3. Kaplan, E. D., "Understanding GPS Principles and Applications", ARTECH HOUSE, Norwood, 1996.
4. Pratap Misra, Per Enge, "Global positioning System" , Ganga-Jamuna Press, Lincoln, 2001.
5. R. Mardiana and Z. Kawasaki, "Broadband radio interferometer utilizing sequential triggering technique for locating fast-moving electromagnetic sources emitted from lightning", IEEE Transactions on Instrumentation and Measurement, vol. 49, no. 2, pp. 376-381, April 2000.
6. L. Cong and W. Zhuang, "Hybrid TDOA/AOA Mobile User Location for Wideband CDMA Cellular Systems", IEEE Transactions on Wireless Communications, vol. 1, no 3, pp. 439-447, July 2002.
7. A. Pagès-Zamora, J. Vidal Manzano, and D.H. Brooks, "Closed-form solution for positioning based on angle of arrival measurements", The 13th IEEE Int. Symposium Personal, Indoor and Mobile Radio Communication, vol. 4, pp. 1522-1526, Sep 2002.
8. Parkinson, B. W., Spilker, J., Jr., Axelrad, P., (eds.), "Global Positioning :Theory and Applications", vol. 1, AIAA, Washington, DC, 1996.
9. D. J. Torrieri, "Statistical Theory of Passive Location Systems", IEEE Transactions on Aerospace and Electronic Systems, vol. AES-20, pp. 183-198, Mar 1984.
10. Börje Forssell, "Radio navigation systems", Prentice Hall, 1991